Research paper

Fire intensity impacts on physiological performance and mortality in *Pinus monticola* and *Pseudotsuga menziesii* saplings: a dose–response analysis

Aaron M. Sparks[1,8], Alexander S. Blanco[1], David R. Wilson[2], Dylan W. Schwilk[3], Daniel M. Johnson[4], Henry D. Adams[5], David M.J.S. Bowman[6], Douglas D. Hardman[1] and Alistair M.S. Smith[1,7]

[1]Department of Forest, Rangeland, and Fire Sciences, College of Natural Resources, University of Idaho, Moscow, ID 83844, USA; [2]Moscow High School, Moscow, ID 83843, USA; [3]Department of Biological Sciences, Texas Tech University, Lubbock, TX 79409, USA; [4]Warnell School of Forestry and Natural Resources, University of Georgia, Athens, GA 30602, USA; [5]School of the Environment, Washington State University, Pullman, WA 99164, USA; [6]School of Natural Sciences, University of Tasmania, Hobart 7001, Australia; [7]Department of Earth and Spatial Sciences, College of Science, University of Idaho, Moscow, ID 83844, USA; [8]Corresponding author (asparks@uidaho.edu)

Fire is a major cause of tree injury and mortality worldwide, yet our current understanding of fire effects is largely based on ocular estimates of stem charring and foliage discoloration, which are error prone and provide little information on underlying tree function. Accurate quantification of physiological performance is a research and forest management need, given that declining performance could help identify mechanisms of—and serve as an early warning sign for—mortality. Many previous efforts have been hampered by the inability to quantify the heat flux that a tree experiences during a fire, given its highly variable nature in space and time. In this study, we used a dose–response approach to elucidate fire impacts by subjecting *Pinus monticola* var. *minima* Lemmon and *Pseudotsuga menziesii* (Mirb.) Franco var. glauca (Beissn.) Franco saplings to surface fires of varying intensity doses and measuring short-term post-fire physiological performance in photosynthetic rate and chlorophyll fluorescence. We also evaluated the ability of spectral reflectance indices to quantify change in physiological performance at the individual tree crown and stand scales. Although physiological performance in both *P. monticola* and *P. menziesii* declined with increasing fire intensity, *P. monticola* maintained a greater photosynthetic rate and higher chlorophyll fluorescence at higher doses, for longer after the fire. *Pinus monticola* also had complete survival at lower fire intensity doses, whereas *P. menziesii* had some mortality at all doses, implying higher fire resistance for *P. monticola* at this life stage. Generally, individual-scale spectral indices were more accurate at quantifying physiological performance than those acquired at the stand-scale. The Photochemical Reflectance Index outperformed other indices at quantifying photosynthesis and chlorophyll fluorescence, highlighting its potential use to quantify crown scale physiological performance. Spectral indices that incorporated near-infrared and shortwave infrared reflectance, such as the Normalized Burn Ratio, were accurate at characterizing stand-scale mortality. The results from this study were included in a conifer cross-comparison using physiology and mortality data from other dose–response studies. The comparison highlights the close evolutionary relationship between fire and species within the *Pinus* genus, assessed to date, given the high survivorship of *Pinus* species at lower fire intensities versus other conifers.

Keywords: chlorophyll fluorescence, fire, fire severity, mortality, photosynthesis, recovery.

Introduction

Fire is one of the major causes of tree injury and mortality in many areas of the world, including western United States forests (Berner et al. 2017, Huo et al. 2019). Heat-induced damage that trees incur during fires can result in significant changes in physiological function, including reduced photosynthesis, phloem dysfunction, and mortality of the cambium and phloem (Smith et al. 2017, Bär et al. 2019, Partelli-Feltrin et al. 2021, 2023). These tree-level impacts, when aggregated to the stand and forest scale, can substantially alter the ecosystem goods and services that forests provide, including hydrologic processes, food and forest products, and protection of soil and biodiversity, among many others (Bonan 2008, Smith et al. 2014, Oswalt et al. 2019). With a warming climate, fire seasons have lengthened (Jolly et al. 2015), and increased fire activity is projected for western United States ecosystems (Abatzoglou et al. 2021, Anderegg et al. 2022). Along with projected increases in wildfire activity, there are growing calls for more prescribed fires to be implemented in forest management plans to reduce hazardous fuel loads (Kolden 2019, Schultz et al. 2019, Hiers et al. 2020, Prichard et al. 2021). Given the projected fiery future, an improved understanding of how tree physiology and mortality are affected by fire is essential for the sustainable management of these forest ecosystems (Shuman et al. 2022).

Fire-induced impacts to tree physiology are a direct consequence of heat flux to the tree crown, stem and roots (Michaletz and Johnson 2007, Bär et al. 2019). In tree stems, tissues that are closer to the bark surface and thus closer to the source of heat (e.g., cambium, phloem) receive higher doses of heat (Butler and Dickinson 2010), which can result in cambium necrosis (Jones et al. 2006) and phloem dysfunction and death (Partelli-Feltrin et al. 2022). Xylem tissues in tree stems are more insulated from heat flux, and studies that utilize actual fires have found that even lethal doses of heat do not affect, or have little effect on, xylem hydraulic function (Battipaglia et al. 2016, Partelli-Feltrin et al. 2021, 2022). This is contrary to experiments that utilize fire proxies (e.g., ovens, hot water baths), where xylem hydraulic function in excised branch segments has been significantly reduced by heat-induced xylem embolism (Michaletz et al. 2012, West et al. 2016, Bär et al. 2018). Beyond tree stems, damage to foliage in tree crowns is of particular importance as this can impair carbon acquisition and lead to reduced non-structural carbohydrate stores needed for growth, maintenance and defense (Smith et al. 2017, Hood et al. 2018a, Sparks et al. 2018, Partelli-Feltrin et al. 2020, 2022, Varner et al. 2021). Foliage exposed to high doses of heat can experience immediate tissue necrosis or be directly combusted (Michaletz and Johnson 2006). Hot gasses from fire plumes can directly impact crowns, leading to bud damage, reduced growth and mortality (Bison et al. 2022). Lower doses of heat to foliage can damage the photosynthetic pathway and

reduce carbon acquisition (Smith et al. 2017, Partelli-Feltrin et al. 2020). In some cases, undamaged foliage on trees with large foliage loss can have greater rates of photosynthesis, likely due to improved water availability for remaining leaves (Wallin et al. 2003, Sayer et al. 2020).

A major challenge of assessing fire effects on tree physiological performance is the heterogenous nature of fire behavior, which results in a heat flux to tree components that is highly variable in space and time (Sparks et al. 2017, O'Brien et al. 2018). To address this issue, many experimental studies have utilized fire proxies, such as convection ovens (West et al. 2016), radiant heaters (Jiménez et al. 2017) and hot water baths (Michaletz et al. 2012, West et al. 2016, Bär et al. 2018). However, the ability of these methods to produce heat fluxes similar to those in actual fires has been questioned (Varner et al. 2021), given that no heat flux comparison studies have been done. Other studies have used a toxicological dose–response approach for characterizing fire intensity effects on tree physiology and mortality (e.g., Smith et al. 2016, 2017, Sparks et al. 2016, 2017, 2018, Steady et al. 2019, Partelli-Feltrin et al. 2020, 2021, 2022), where fire intensity represents the energy released (i.e., heat flux) during the various combustion phases of fire (Keeley 2009). Using this dose–response approach, trees are subjected to actual fires with a known fire intensity (dose) reported as the total radiative heat flux incident on a tree or fire radiative energy (FRE, units: MJ m^{-2}). Tree physiological impacts (responses) are assessed pre- and post-fire. The use of consistent and repeatable doses of heat from actual fires provides a promising approach to assessing fire effects (Hood et al. 2018a, O'Brien et al. 2018); however, large knowledge gaps remain, as only a few tree species of limited size have been assessed using this approach.

Quantifying the physiological performance of fire-affected tree foliage is a forest management research need (Smith et al. 2016, Varner et al. 2021), given that reduced performance could serve as an early indicator of tree death (Sperry and Love 2015, Hood et al. 2018a). However, most assessments of tree crowns after fire are limited to subjective ocular estimations of tree crown damage, termed 'crown scorch', which provide limited insight into the physiological status of the tree crown (Smith et al. 2016, Sparks et al. 2016, Varner et al. 2021). Instead, assessments that provide information about the state of photosynthetic machinery and carbon assimilation in tree foliage may provide mechanistic and scalable metrics, given decreased photosynthetic activity for extended periods can reduce non-structural carbon reserves and lead to carbon starvation and death (McDowell et al. 2011, Bär et al. 2019, Partelli-Feltrin et al. 2022). Prior studies have shown that greater heat-induced damage to conifer saplings results in lower stomatal conductance, net photosynthesis and chlorophyll fluorescence, and in greater mortality (Smith et al. 2017, Steady et al. 2019, Partelli-Feltrin et al. 2022). Remote sensing of foliar spectral reflectance

provides an avenue for assessing physiological function and the water and chemical content of crown foliage (Choudhury 1987, Gamon et al. 1992, Asner et al. 2015, Gamon et al. 2016); however, little work has explored the potential of assessing physiological change in burned trees. For example, Sparks et al. (2016) observed that spectral indices derived from leaf-level spectral reflectance accurately characterized photosynthesis and chlorophyll fluorescence in burned *Pinus contorta* var. *latifolia* and *Larix occidentalis* sapling foliage. It is not known if these relationships would be accurate at larger scales (e.g., stand or landscape scale) due to confounding issues such as complex tree crown illumination conditions and mixed species composition within a forest stand (Williams 1991, Asner et al. 2015).

In this study, the overall objective was to assess short-term effects (weeks to months) of fire on physiological performance and mortality in *Pinus monticola* var. *minima* Lemmon and *Pseudotsuga menziesii* (Mirb.) Franco var. *glauca* (Beissn.) Franco saplings and evaluate whether these effects are detectable using spectral reflectance indices. Here, we define sapling as the growth stage following seedlings, where seedlings are plants dependent on stored seed reserves (Thomas and Winner 2002, Brodersen et al. 2019). Specifically, we tested the following hypotheses: (H1) increased fire intensity results in decreased physiological performance and increased mortality in both species and (H2) changes in physiological performance and mortality are detectable using leaf-level and stand-level spectral reflectance indices. To address the overall objective, saplings were subjected to surface fire treatments of known intensity (doses) in a controlled laboratory setting, and physiological performance and mortality (responses) were assessed up to 2 months post-treatment. Photosynthesis, chlorophyll fluorescence and individual- and sapling stand-level spectral reflectance were measured before and after fire treatment. Relationships between fire intensity or spectral reflectance and tree physiology or mortality metrics were assessed using regression modeling. Finally, the results from this study were included in a cross-conifer comparison using physiology and mortality data from other dose–response studies to further understand how responses vary across species.

Materials and methods

Ecology

Pinus monticola var. *minima* (western white pine) is an early seral species found from British Columbia to California and from the Pacific coast to western Montana (Burns and Honkala 1990, Loehman et al. 2011). The species is ecologically important and an important timber species in the United States (Burns and Honkala 1990). The mature trees can live over 400 years and exhibit heights exceeding 60 m and diameter at breast height of 2.4 m (Griffith 1992, Loehman et al. 2011). Mature trees exhibit moderate levels of resistance to fire with thick bark

and high crowns (Loehman et al. 2011), but this resistance decreases as stand density increases (Davis et al. 1980, Burns and Honkala 1990). Although limited fire ecology data exist on young trees, saplings are broadly considered sensitive to fire damage and mortality due to having thin bark (Griffith 1992, Hood et al. 2018b). The literature is inconsistent regarding whether foliage flammability and branch structure in mature trees promote or inhibit crown fires (Burns and Honkala 1990, Loehman et al. 2011).

Pseudotsuga menziesii var. *glauca* (Rocky Mountain Douglas-fir) exists in mountainous regions from central British Columbia to Mexico and from central Washington to eastern Colorado, and is an important timber species throughout its range (Steinberg 2002). Although the species is considered shade intolerant in wet forests, it is categorized as moderately shade tolerant and a climax species in more arid forests (Burns and Honkala 1990). Although mature trees exhibit moderate to high levels of fire resistance through thick insulative bark (Peterson and Arbaugh 1986, Ryan et al. 1988), younger trees are susceptible to fire-induced damage due to thin bark, closely spaced flammable needles and resin blisters located in the bark (Fischer and Bradley 1987, Agee 1993). Norum (1976) observed that small-stemmed (<10 cm diameter) Rocky Mountain Douglas-fir are generally killed by prescribed fires and that strong relationships predictive of mortality could be derived using diameter and fire intensity. Other studies suggest that injury and mortality in this species may arise from the fires damaging the crown (Engber and Varner 2012) and major lateral roots located in the transition between the organic and mineral soil layers (Ryan et al. 1988).

Pinus and Pseudotsuga saplings and study treatments

Pinus monticola ($n = 35$) and *P. menziesii* saplings ($n = 35$) were grown in 9.5-l pots through two growing seasons under natural light conditions in a climate-controlled greenhouse in Moscow, Idaho, USA (46.73°N, 117.0°W). During this period, saplings were watered to field capacity daily to minimize water stress. Immediately prior to fire treatments, average (±SE) root collar diameters were 1.83 ± 0.04 cm and 2.10 ± 0.05 cm and mean heights were 0.73 ± 0.27 m and 0.99 ± 0.28 m for *P. monticola* and *P. menziesii*, respectively.

In June of 2021, *P. monticola* and *P. menziesii* saplings were randomly divided into five groups ($n = 7$): (i) control saplings that were not burned; (ii) saplings subjected to a surface fire with FRE of 0.4 MJ m^{-2}; (iii) saplings subjected to a surface fire with FRE of 0.6 MJ m^{-2}; (iv) saplings subjected to a surface fire with FRE of 0.8 MJ m^{-2}; and (v) saplings subjected to a surface fire with FRE of 1 MJ m^{-2}. Fire radiative energy was used as the dose metric, given that prior studies have shown that pure fuel beds with the same mass and moisture content produce consistent and repeatable quantities of FRE (Smith et al. 2013, 2016, Wooster et al. 2021). The specific doses were created by burning fuelbeds of pure *P. monticola* needles at <1% moisture

content. Following Smith et al. (2013, 2017), the following relationship between fuel load and FRE was used to calculate the necessary fuel load for each dose group: *P. monticola* needle fuel load (kg) = 2.679/FRE. Saplings in each dose group were inserted into a custom cut concrete board so that the soil surface of the sapling pot was level with the board. The corresponding fuel load of dry needles was evenly distributed in a 1 m^2 circular area surrounding each sapling and ignited on one side to produce a surface fire with a uniform flaming front. After the fire treatment, saplings were watered to field capacity daily. The experiment was a completely randomized design, and saplings were rearranged weekly to minimize environmental variation associated with sapling position.

Photosynthesis and chlorophyll fluorescence measurements

Light-saturated gas exchange measurements were acquired on five randomly selected saplings in each FRE dose group with a LI-6800 portable photosynthesis system (LI-COR Biosciences, Lincoln, NE, USA). Measurements included light-saturated net photosynthesis (A_{max}) and stomatal conductance to water vapor (g_s) and were performed with a constant photosynthetic flux of 1500 μmol m^{-2} s^{-1} and CO_2 level of 400 p.p.m. Measurements were taken 1 day before the fire treatments, which occurred in the first week of July, and at 28 days and 56 days after the fire treatments between 10 a.m. and 12 p.m. The average air temperature was 33.7 and 31.0 °C, and the relative humidity was 36.3 and 32.8% at 28 and 56 days post-fire, respectively. Gas exchange measurements were taken on needles that had survived the fire (i.e., needles with minimal visible damage or discoloration) in the top one-third of each sapling crown. Measurements were taken on mature needles that had been produced in the previous year. If a selected sapling only had brown needles, no gas exchange measurements were acquired. Needles were marked to indicate the proportion of the needles inside the leaf chamber. After gas exchange measurement, each marked needle group was photographed on a white background with a measurement scale for reference using an 18-megapixel Canon Powershot camera (Canon USA, Inc., Melville, NY, USA). Images were cropped using the needle markings, and total leaf area (cm^2) was calculated using ImageJ software (v.1.53; developed by W.S. Rasband, US National Institutes of Health, Bethesda, MD, USA). Leaf area estimates and gas exchange data were used to calculate net photosynthesis on a leaf area basis. Relative net photosynthesis was also calculated as: $[((A_{postfire} - A_{prefire})/A_{prefire}) \times 100]$.

Chlorophyll fluorescence measurements were acquired on all study trees on the same post-fire days as the gas exchange measurements, using an OS30p + fluorometer (Opti-Sciences, Hudson, NH, USA). Measurements were acquired at least 1 h after sunset so that needles could dark adapt. For each sapling, minimal fluorescence (F_o) was measured, and maximum fluorescence (F_m) was measured after a short saturation pulse

(3500 μmol m^{-2} s^{-1}) of red light centered at 660 nm. Maximum quantum yield of photosystem II (F_v/F_m) was calculated following Genty et al. (1989):

$$\frac{F_v}{F_m} = \frac{F_m - F_o}{F_m}$$

Spectral reflectance measurements and spectral indices

Spectral reflectance was measured on the same saplings and sample dates as the gas exchange and chlorophyll fluorescence measurements, using an ASD FieldSpec Pro spectroradiometer (Malvern Panalytical Ltd, Malvern, UK). This spectroradiometer collects measurements at wavelengths between 350 and 2500 nm and has a spectral resolution of 3 nm between 350 and 1000 nm and 10 nm between 1000 and 2500 nm. Individual sapling spectra were acquired in the top one-third of each sapling. Radiance measurements were calibrated using a 100% reflective Lambertian Spectralon panel (Labsphere Inc., North Sutton, NH, USA) before each scan. Three spectral scans were acquired for each sapling using the mineral probe attachment to minimize noise due to the absorption of water vapor in the air. For each scan, the instrument acquired and averaged 10 spectra to reduce noise.

Spectra of sapling stands were collected by arranging the five selected saplings in each FRE dose group into synthetic 'stands', which provided a semi-closed canopy (Figure 1). Saplings were positioned on a spectrally flat, charred concrete board (i.e., covered in charcoal residue), which provided a realistic background for the stand scale spectral scans. Spectral scans were acquired at 2.31 m above the burn board using the fiber optic cable with a 25° field of view. All stand spectra were acquired outside between 10 a.m. and 12:00 p.m. so that illumination conditions were similar between dose groups. Three spectral scans were acquired for each group, and the saplings were rotated 90° between each scan. Images of each sapling stand were taken pre- and post-fire at nadir and at the same height as stapling stand spectra measurements using an 18-megapixel Canon Powershot camera (Canon USA, Inc., Melville, NY, USA) (Figure 1). All individual and stand spectra were processed via linear interpolation to 1 nm resolution, resulting in 2151 spectral bands, before any further spectral processing was performed.

The spectral reflectance measurements were used to calculate spectral indices demonstrated to be sensitive to vegetation physiology and/or live canopy cover (Table 1). For spectral indices that do not use specific wavelengths, spectra were converted to band-equivalent reflectance (Trigg and Flasse 2000, Smith et al. 2005) associated with the Landsat 8 satellite sensor, given the widespread use of Landsat 8 to map live vegetation cover and post-fire mortality (McCarley et al. 2017, Furniss et al. 2020, Tyukavina et al. 2022). The Chlorophyll/Carotenoid Index (CCI) (Gamon et al. 2016), Photochemical Reflectance Index
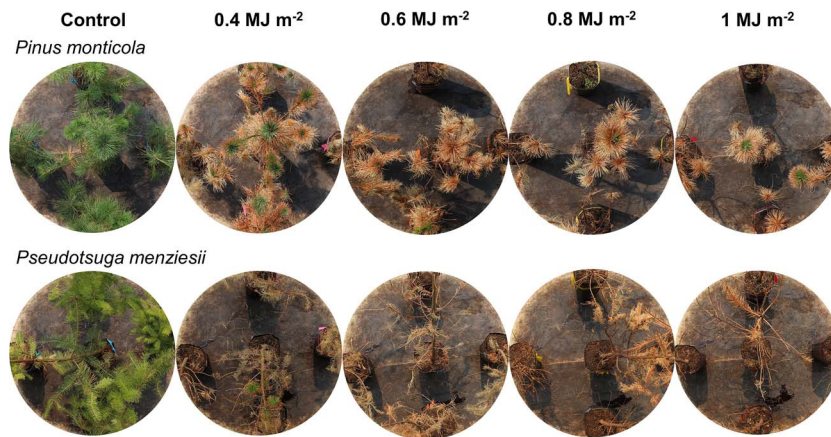
Figure 1. Photos of *Pinus monticola* (top row) and *Pseudotsuga menziesii* (bottom row) dose groups taken at nadir 28 days post-fire. Photos are cropped to the approximate field-of-view of the spectroradiometer.

(PRI) (Gamon et al. 1992) and Normalized Difference Vegetation Index (NDVI) (Rouse et al. 1974) have been demonstrated in prior studies to accurately characterize photosynthesis and chlorophyll fluorescence (Carter 1998, Peñuelas et al. 2011, Sparks et al. 2016, Wong et al. 2019). Spectral indices including the Char Soil Index (CSI) (Smith et al. 2005), Mid-infrared Burn Index (MIRBI) (Trigg and Flasse 2001), Normalized Burn Ratio (NBR) (Key and Benson 2006), the Relativized differenced Normalized Burn Ratio (RdNBR) (Miller and Thode 2007), SWIR2-NIR band ratio (Kushla and Ripple 1998) and SWIR2-SWIR1 band ratio (Epting 2005) have been shown to accurately quantify live canopy cover change and mortality in prior studies (Miller and Thode 2007, Sparks et al. 2016, McCarley et al. 2017, Furniss et al. 2020). Differenced formulations were calculated for all spectral indices to capture changes pre- to post-fire and were calculated as the difference between the pre-fire spectral index value and post-fire spectral index value. These formulations are noted with a 'd' before the spectral index abbreviation.

Data analysis

Relationships between FRE or each spectral index and tree physiology or mortality metrics were assessed using regression modeling, where physiology metrics (A_{max}, g_s, relative A, F_v/F_m) were the response variables, and FRE or spectral indices (Table 1) were the predictor variables. Relationships were assessed separately for each species, post-fire sampling date (28 and 56 days post-fire) and scale (individual and stand). Regression modeling was conducted using the 'DoseFinding' (Bornkamp et al. 2022) and 'nlme' (Pinheiro and Bates 2022) R packages in R statistical software (R Core Team 2022). Prior studies have indicated that the form of the relationship between FRE or spectral indices and tree physiology and mortality can vary. For example, Sparks et al. (2016) and Smith et al. (2017) observed a linear relationship between

FRE or spectral indices and net photosynthesis in *P. contorta* (Douglas) and *L. occidentalis* (Nutt.) saplings. Others have observed sigmoidal relationships between FRE and mortality in *P. contorta* (Douglas) and *Pinus ponderosa* (Dougl. ex Laws) saplings (Smith et al. 2017, Steady et al. 2019). Given this variability, we assessed several regression models for each predictor and response variable pair, and the best fit for models that were significant ($\alpha = 0.05$) was determined by the lowest Akaike Information Criterion (AIC) value (Akaike 1974). For each best fit model, the residual standard error (SE) and the coefficient of determination (r^2) for linear models were computed and used to evaluate the relationship 'goodness of fit'. Assessed regression models are shown in Table 2.

The results from this study were included in a conifer cross-comparison using A_{max} and mortality data from other published dose–response studies. The included studies used similarly sized and aged saplings (~2–3 years old) and a similar range of FRE doses. Selected studies assessed dose–response relationships for the following species: *P. ponderosa* (Dougl. ex Laws.) (Steady et al. 2019), *P. contorta* (Douglas) (Smith et al. 2017) and *L. occidentalis* (Nutt.) (Smith et al. 2017).

Results

Physiology and mortality dose–response

A_{max}, relative A and g_s for both species generally decreased with increasing FRE at 28 and 56 days post-fire (Figures 2a–c and 3a–c). The Sigmoid E_{max} regression model provided the best fit (lowest AIC) for dose–response relationships between FRE and A_{max} at 28 days post-fire for *P. monticola* ($P < 0.001$, AIC: 43.5) and *P. menziesii* ($P < 0.001$, AIC: 67.8) (Tables S1 and S5 available as Supplementary data at *Tree Physiology* Online) and at 56 days post-fire for *P. monticola* ($P < 0.001$, AIC: 63.5) (Tables S2 and S6 available as Supplementary data at *Tree Physiology* Online). Relationships between FRE and relative

Table 1. Spectral index formulation and associated reference.

Spectral Index	Formula	Reference
CCI	$(\rho_{531} - \rho_{645})/(\rho_{531} + \rho_{645})$	Gamon et al. 2016
Differenced CCI (dCCI)	$(CCI_{pre\text{-}fire} - CCI_{post\text{-}fire})$	
CSI	ρ_{NIR}/ρ_{SWIR1}	Smith et al. 2005
Differenced CSI (dCSI)	$(CSI_{pre\text{-}fire} - CSI_{post\text{-}fire})$	
MIRBI	$10 \times \rho_{SWIR2}\text{-}9.8 \times \rho_{SWIR1} + 2$	Trigg and Flasse 2001
Differenced MIRBI (dMIRBI)	$(MIRBI_{pre\text{-}fire} - MIRBI_{post\text{-}fire})$	
NDVI	$(\rho_{NIR} - \rho_{red})/(\rho_{NIR} + \rho_{red})$	Rouse et al. 1974
Differenced NDVI (dNDVI)	$(NDVI_{pre\text{-}fire} - NDVI_{post\text{-}fire})$	
NBR	$(\rho_{NIR} - \rho_{SWIR2})/(\rho_{NIR} + \rho_{SWIR2})$	Key and Benson 2006
Differenced NBR (dNBR)	$(NBR_{pre\text{-}fire} - NBR_{post\text{-}fire})$	
Relativized differenced NBR	$dNBR/(|NBR_{pre\text{-}fire}|/1000)^{0.5}$	Miller and Thode 2007
PRI	$(\rho_{531} - \rho_{570})/(\rho_{531} + \rho_{570})$	Gamon et al. 1992
Differenced PRI (dPRI)	$(PRI_{pre\text{-}fire} - PRI_{post\text{-}fire})$	
SWIR2-NIR band ratio (SW2NIR)	ρ_{SWIR2}/ρ_{NIR}	Kushla and Ripple 1998
Differenced SW2NIR (dSW2NIR)	$(SW2NIR_{pre\text{-}fire} - SW2NIR_{post\text{-}fire})$	
SWIR2-SWIR1 band ratio (SW2SW1)	$\rho_{SWIR2}/\rho_{SWIR1}$	Epting et al. 2005
Differenced SW2SW1 (dSW2SW1)	$(SW2SW1_{pre\text{-}fire} - SW2SW1_{post\text{-}fire})$	

ρ_λ denotes reflectance in spectral band λ. ρ_{red} = red reflectance, ρ_{NIR} = near infrared reflectance, ρ_{SWIR} = short-wave infrared reflectance.

Table 2. Regression model formulae used in the analysis of relationships between FRE or each spectral index and tree physiology or mortality.

Regression model	Formula
Linear	$y = mx + b$
Quadratic	$y = b + \beta_1 x + \beta_2 x^2$
E_{max}	$y = E_0 + E_{max}\frac{x}{ED_{50}+x}$
Sigmoid E_{max}	$y = E_0 + E_{max}\frac{x^h}{ED_{50}^h+x^h}$

Model coefficients are as follows: m = slope, b = y-intercept, β_x = quadratic fit coefficients, E_0 = left asymptote parameter for sigmoidal fits, E_{max} = asymptotic maximum effect, ED_{50} = value giving half of the asymptotic maximum effect, h = hill parameter that determines the steepness of the model at ED_{50}.

A were similar to FRE–A_{max} relationships, although models with the best fit differed (Figures 2b and 3b). Dose–response relationships between FRE and g_s varied between the species. At 28 and 56 days post-fire, quadratic ($P < 0.001$, AIC: −83.7) and linear ($P < 0.001$, AIC: −69.6) models provided the best fit for the FRE-g_s relationship in *P. monticola*, respectively (Figure 2c; Tables S1 and S2, S5 and S6 available as Supplementary data at *Tree Physiology* Online). In contrast, Sigmoid E_{max} regression models provided the best fit for the FRE–g_s relationship in *P. menziesii* at 28 days ($P < 0.001$, AIC: −62.8) and 56 days ($P < 0.001$, AIC: −55.7) post-fire (Figure 3c; Tables S1, S2, S5 and S6 available as Supplementary data at *Tree Physiology* Online).

Chlorophyll fluorescence (F_v/F_m) dose–response relationships differed between the two species. Burned *P. monticola* generally maintained higher F_v/F_m values at 28 days post-fire compared with *P. menziesii* (Figures 2d and 3d). *Pinus monticola*

displayed a sigmoidal decrease in F_v/F_m with increasing FRE (Figure 2d), with Sigmoid E_{max} models providing the best fit at 28 days ($P < 0.001$, AIC: 8.4) and 56 days ($P < 0.001$, AIC: −3.3) post-fire (Tables S1, S2, S5 and S6 available as Supplementary data at *Tree Physiology* Online). In contrast, *P. menziesii* displayed decreases in F_v/F_m at all FRE doses (Figure 3d), with linear and Sigmoid E_{max} models providing the best fit at 28 days ($P < 0.001$, AIC: −0.3) and 56 days ($P < 0.001$, AIC: −8.1) post-fire (Tables S1, S2, S5 and S6 available as Supplementary data at *Tree Physiology* Online).

Mortality increased with increasing FRE dose for both species (Figures 2e and 3e). Sigmoid E_{max} regression models provided the best fit (lowest AIC) for dose–response relationships between FRE and mortality for *P. monticola* and *P. menziesii* at 28 days post-fire ($P < 0.001$, AIC: 22.8 and $P < 0.001$, AIC: 22.2, respectively) and at 56 days post-fire ($P < 0.001$, AIC: 27.7 and $P < 0.001$, AIC: 10.4, respectively) (Tables S1 and S2, S5 and S6 available as Supplementary data at *Tree Physiology* Online). The lowest observed adverse effect level for mortality was observed to be 0.4 MJ m^{-2} for *P. menziesii* and 0.6 MJ m^{-2} for *P. monticola*. Delayed mortality resulted in a leftward shift of the relationship fit from 28 days post-fire to 56 days post-fire for both *P. monticola* and *P. menziesii* (Figures 2e and 3e).

Spectral characterization of physiological performance and mortality

Figure 4 displays the regression relationships between individual sapling physiological metrics and spectral indices that yielded the lowest AIC value, and therefore, represent the best fitting predictive model among the four models that were tested.
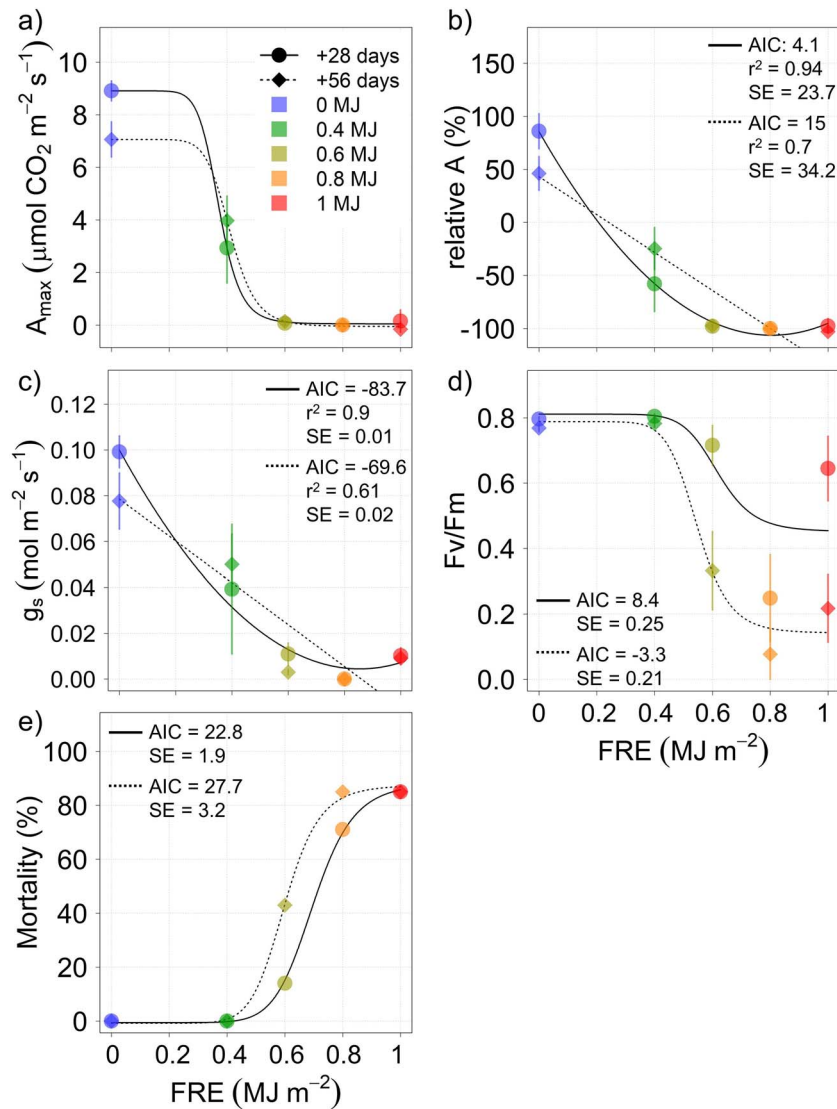
Figure 2. Dose–response relationships between FRE and *P. monticola* physiology or mortality at 28 days post-fire (circles) and 56 days post-fire (diamonds). Panels show dose–response relationships between FRE dose and response variables: (a) light-saturated net photosynthesis (A_{max}), (b) relative net photosynthesis, (c) stomatal conductance to water vapor (g_s), (d) chlorophyll fluorescence (F_v/F_m) and (e) mortality. Mean values $\pm$ SE are shown in panels (a) to (d). Colors represent FRE doses: blue = 0 MJ m^{-2}, green = 0.4 MJ m^{-2}, yellow = 0.6 MJ m^{-2}, orange = 0.8 MJ m^{-2} and red = 1 MJ m^{-2}. The regression model fits with the lowest AIC are also displayed for data at 28 days post-fire (solid line) and 56 days post-fire (dotted line). The residual SE and coefficient of determination (r^2) for linear models are also reported. SE for panel (a) is 0.79 and 1.5 for data at 28 and 56 days post-fire, respectively.

For both species, the best fit regression models were linear models utilizing the PRI and CCI spectral indices for predicting A_{max} and relative A (Figure 4; Tables S1 and S2 available as Supplementary data at *Tree Physiology* Online). Generally, higher values of PRI and CCI corresponded with higher values of A_{max} and relative A (Figure 4). For *P. monticola*, PRI was the best predictor of A_{max} ($P < 0.001$, AIC: 57.1) and relative A ($P < 0.001$, AIC: 143.2) at 28 days post-fire, and CCI was the best predictor of A_{max} ($P < 0.001$, AIC: 57.6) and relative A ($P < 0.001$, AIC: 136.6) at 56 days post-fire (Tables S1, S2, S7 and S8 available as Supplementary data at *Tree Physiology* Online). Spectral indices dPRI and dCCI provided the next best fits for

prediction of A_{max} ($P < 0.001$, AIC: 63.4 and $P < 0.001$, AIC: 65.5, respectively) and relative A at 28 days post-fire ($P < 0.001$, AIC: 148.2 and $P < 0.001$, AIC: 148.2, respectively) (Tables S7 and S8 available as Supplementary data at *Tree Physiology* Online). Similarly, spectral indices PRI and dCCI provided the next best fits for prediction of A_{max} ($P < 0.001$, AIC: 58.8 and $P < 0.001$, AIC: 58.6, respectively) and relative A at 56 days post-fire ($P < 0.001$, AIC: 138.9 and $P < 0.001$, AIC: 136.7, respectively) (Tables S7 and S8 available as Supplementary data at *Tree Physiology* Online). For *P. menziesii*, PRI was the best predictor of A_{max} ($P < 0.001$, AIC: 37.0) and relative A ($P < 0.01$, AIC: 95.7) at 28 days post-fire, and was
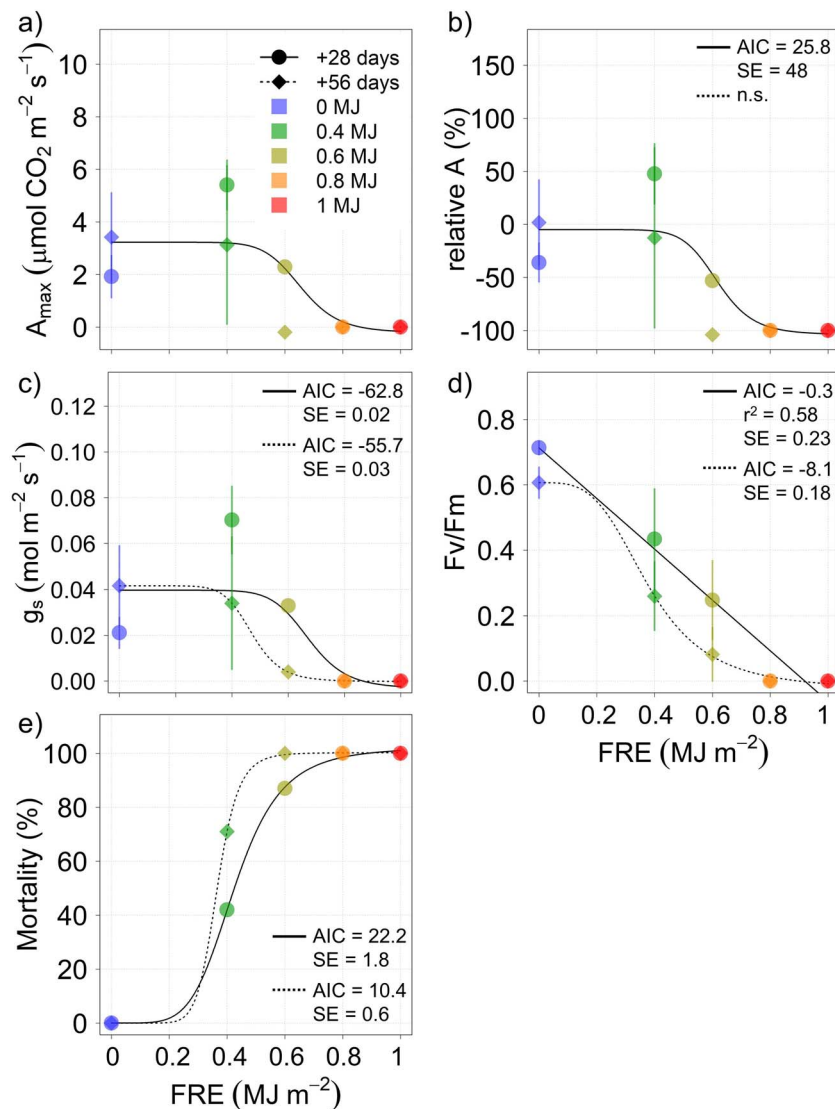
Figure 3. Dose–response relationships between FRE and *P. menziesii* physiology or mortality at 28 days post-fire (circles) and 56 days post-fire (diamonds). Panels show dose–response relationships between FRE dose and response variables: (a) light-saturated net photosynthesis (A_{max}), (b) relative net photosynthesis, (c) stomatal conductance to water vapor (g_s), (d) chlorophyll fluorescence (F_v/F_m), and (e) mortality. Mean values ± SE are shown in panels (a) to (d). Colors represent FRE doses: blue = 0 MJ m^{-2}, green = 0.4 MJ m^{-2}, yellow = 0.6 MJ m^{-2}, orange = 0.8 MJ m^{-2} and red = 1 MJ m^{-2}. The regression model fits with the lowest AIC are also displayed for data at 28 days post-fire (solid line) and 56 days post-fire (dotted line). Instances where none of the regression models were significant are denoted as (n.s.). The residual SE and coefficient of determination (r^2) for linear models are also reported. SE for panel (a) is 1.94 for data at 28 days post-fire.

also the best predictor of A_{max} ($P < 0.001$, AIC: 45.5) and relative A ($P < 0.01$, AIC: 101.9) at 56 days post-fire (Figure 4b and d; Tables S1, S2, S7 and S8 available as Supplementary data at *Tree Physiology* Online). Spectral indices dPRI and NDVI provided the next best fits at 28 days post-fire for prediction of A_{max} ($P < 0.001$, AIC: 42.2 and $P < 0.001$, AIC: 43.8, respectively) and relative A ($P < 0.001$, AIC: 99.7 and $P < 0.001$, AIC: 101.7, respectively) (Tables S7 and S8 available as Supplementary data at *Tree Physiology* Online). At 56 days post-fire, spectral indices dPRI and CCI provided the next best fits for prediction of A_{max} ($P < 0.001$, AIC: 46.9 and $P < 0.001$, AIC: 49.3, respectively) and relative A ($P < 0.001$, AIC: 103.6

and $P < 0.001$, AIC: 106.1, respectively) (Tables S7 and S8 available as Supplementary data at *Tree Physiology* Online).

Regression relationships between F_v/F_m and spectral indices with the lowest AIC values are shown in Figure 4e and f. All of the best fit models used a linear fit for both species. For *P. monticola*, PRI was the best predictor of F_v/F_m at 28 days post-fire ($P < 0.001$, AIC: −56.9) and at 56 days post-fire ($P < 0.01$, AIC: −32.5) (Figure 4e; Tables S1, S2, S7 and S8 available as Supplementary data at *Tree Physiology* Online). Spectral indices dPRI and dMIRBI provided the next best fits for prediction of F_v/F_m at 28 days post-fire ($P < 0.001$, AIC: −55.4 and $P < 0.001$, AIC: −54.9, respectively), and
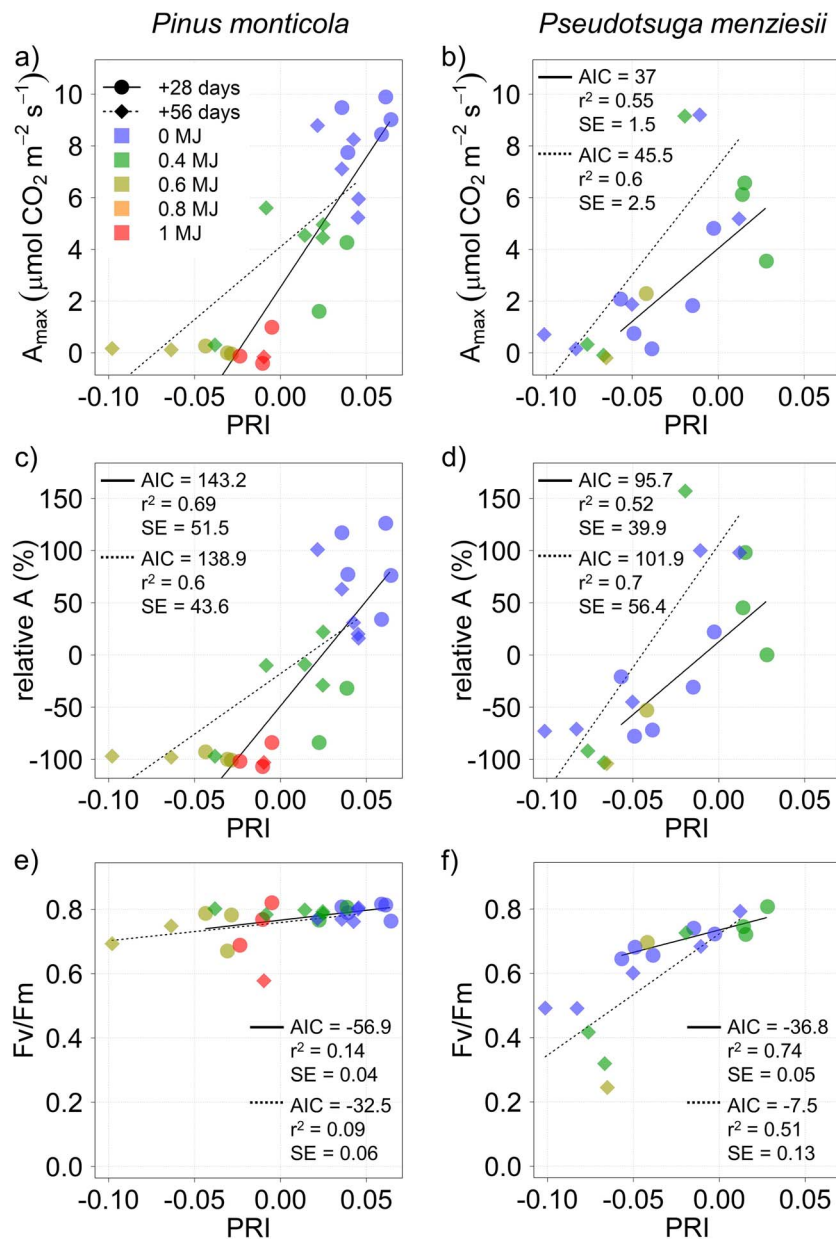
Figure 4. Relationships between spectral indices derived from individual sapling spectral reflectance measurements and (a, b) light-saturated net photosynthesis (A_{max}), (c, d) relative photosynthesis and (e, f) chlorophyll fluorescence (F_v/F_m) at 28 days post-fire (circles) and 56 days post-fire (diamonds). Each data point represents the average of three spectral scans with colors representing FRE doses: blue = 0 MJ m^{-2}, green = 0.4 MJ m^{-2}, yellow = 0.6 MJ m^{-2}, orange = 0.8 MJ m^{-2} and red = 1 MJ m^{-2}. The regression model fits with the lowest AIC are displayed on each pane. The residual SE and coefficient of determination (r^2) for linear models are also reported. The AIC, r^2 and SE for panel (a) are 57.1, 0.81 and 1.88 for data at 28 days and 58.5, 0.61 and 1.98 for data at 56 days post-fire, respectively.

spectral indices dPRI and MIRBI provided the next best fits for prediction of F_v/F_m at 56 days post-fire ($P < 0.001$, AIC: −32.4 and $P < 0.001$, AIC: −32.3, respectively) (Tables S7 and S8 available as Supplementary data at *Tree Physiology* Online). For *P. menziesii*, PRI was the best predictor of F_v/F_m at 28 days post-fire ($P < 0.001$, AIC: −36.8), and dPRI was the best predictor of F_v/F_m at 56 days post-fire ($P < 0.01$, AIC: −12.3) (Figure 4f; Tables S1, S2, S7 and S8 available as

Supplementary data at *Tree Physiology* Online). Spectral indices dPRI and NDVI provided the next best fits for prediction of F_v/F_m at 28 days post-fire ($P < 0.001$, AIC: −32.0 and $P < 0.05$, AIC: −27.1, respectively), and spectral indices CCI and dCCI provided the next best fits for prediction of F_v/F_m at 56 days post-fire ($P < 0.05$, AIC: −10.8 and $P < 0.001$, AIC: −8.9, respectively) (Tables S7 and S8 available as Supplementary data at *Tree Physiology* Online).
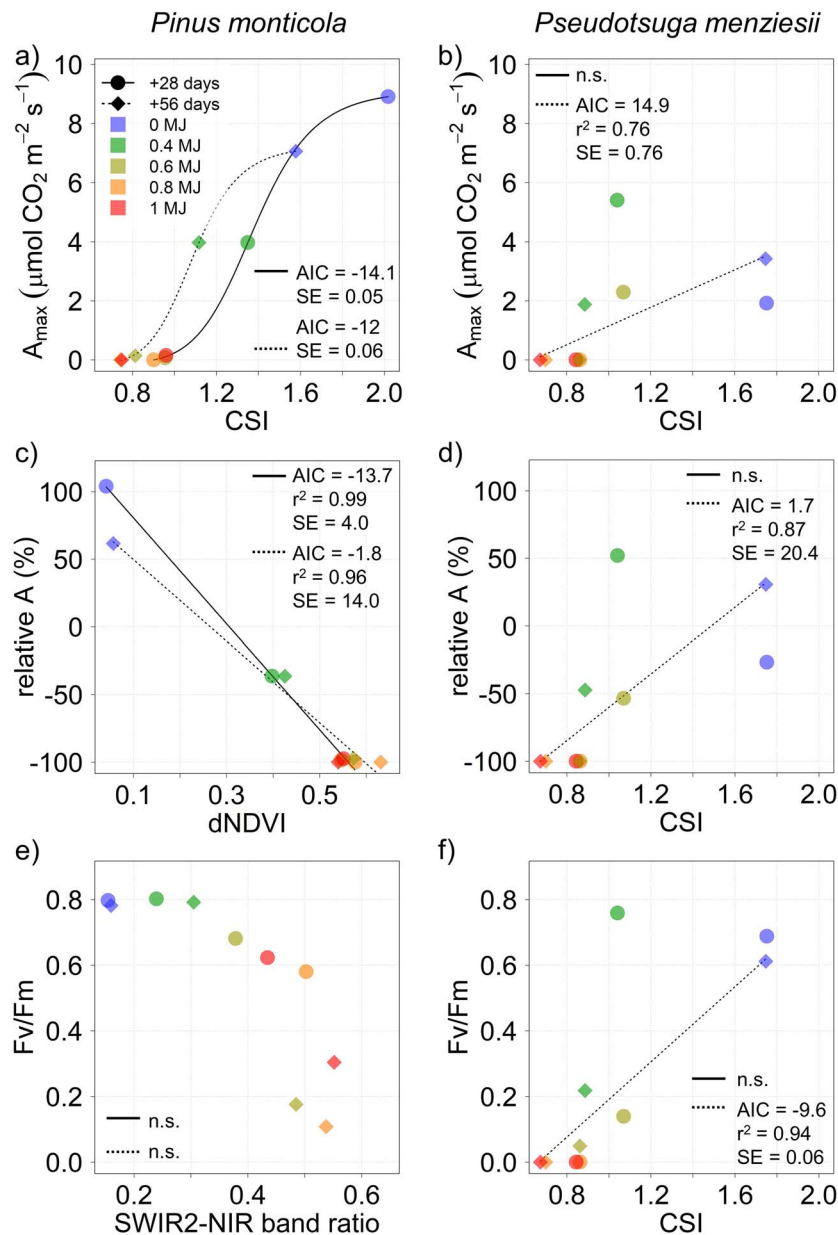
Figure 5. Relationships between spectral indices derived from sapling stand spectral reflectance measurements and stand average (a, b) light-saturated net photosynthesis (A_{max}), (c, d) relative A and (e, f) chlorophyll fluorescence (F_v/F_m) at 28 days post-fire (circles) and 56 days post-fire (diamonds). Each data point represents the average of three spectral scans with colors representing FRE doses: blue = 0 MJ m^{-2}, green = 0.4 MJ m^{-2}, yellow = 0.6 MJ m^{-2}, orange = 0.8 MJ m^{-2} and red = 1 MJ m^{-2}. The regression model fit with the lowest AIC and SE is displayed on each pane. Instances where none of the regression models were significant are denoted as (n.s.). The residual SE and coefficient of determination (r^2) for linear models are also reported.

Figure 5a and b displays the sapling stand relationships between stand A_{max} average and spectral indices. For *P. monticola*, the regression models with the best fit utilized CSI for predicting stand A_{max} average at 28 days post-fire ($P < 0.001$, AIC: −14.1) (Figure 5a) and RdNBR for predicting stand A_{max} average at 56 days post-fire ($P < 0.001$, AIC: −34.1) (Tables S3, S4, S9 and S10 available as Supplementary data at *Tree Physiology* Online). Spectral indices RdNBR and dNBR provided the next best fits for prediction of stand A_{max} average at

28 days post-fire ($P < 0.001$, AIC: −6.4 and $P < 0.001$, AIC: −6.4, respectively), and dNBR and NBR provided the next best fits for prediction of stand A_{max} average at 56 days post-fire ($P < 0.001$, AIC: −30.7 and $P < 0.001$, AIC: −28.9, respectively) (Tables S9 and S10 available as Supplementary data at *Tree Physiology* Online). In terms of predicting relative A, the regression models with the best fit utilized dNDVI at 28 days post-fire ($P < 0.001$, AIC: −13.7) (Figure 5b) and CSI at 56 days post-fire ($P < 0.001$, AIC: −10.6) (Tables S3, S4, S9
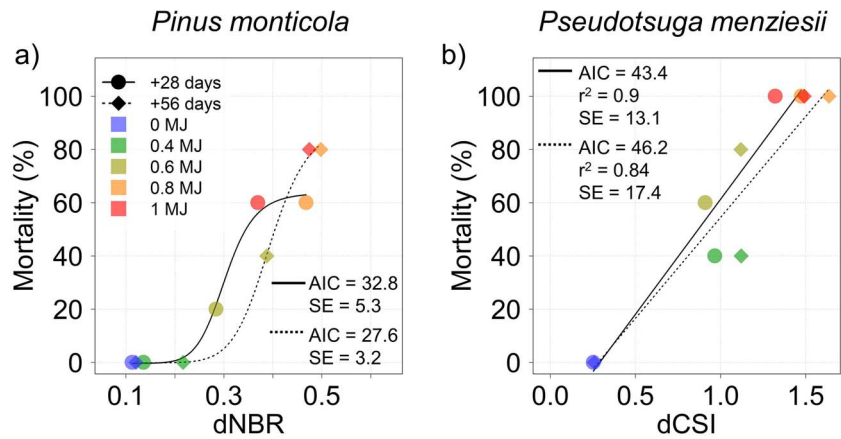
Figure 6. Relationships between spectral indices derived from sapling stand spectral reflectance measurements and mortality at 28 days post-fire (circles) and 56 days post-fire (diamonds). Each data point represents the average of three spectral scans with colors representing FRE doses: blue = 0 MJ m^{-2}, green = 0.4 MJ m^{-2}, yellow = 0.6 MJ m^{-2}, orange = 0.8 MJ m^{-2}and red = 1 MJ m^{-2}. The regression model fit with the lowest AIC and SE is also displayed on each pane. The residual SE and coefficient of determination (r^2) for linear models are also reported.

and S10 available as Supplementary data at *Tree Physiology* Online). Spectral indices CSI and NDVI provided the next best fits for prediction of stand relative A at 28 days post-fire ($P < 0.001$, AIC: -6.9 and $P < 0.001$, AIC: -5.2, respectively), and SW2SW1 and NDVI provided the next best fits for prediction of relative A at 56 days post-fire ($P < 0.001$, AIC: -7.8 and $P < 0.001$, AIC: -2.6, respectively) (Tables S9 and S10 available as Supplementary data at *Tree Physiology* Online). None of the regression models characterizing the relationship between spectral indices and stand average F_v/F_m was significant at 28 or 56 days post-fire (Tables S9 and S10 available as Supplementary data at *Tree Physiology* Online). For *P. menziesii*, the regression models with the best fit utilized CSI for predicting stand A_{max} average at 56 days post-fire ($P < 0.001$, AIC: 14.9) (Figure 5b; Tables S4 and S10 available as Supplementary data at *Tree Physiology* Online). None of the regression models characterizing the relationship between spectral indices and stand A_{max} average was significant at 28 days post-fire (Tables S9 and S10 available as Supplementary data at *Tree Physiology* Online). Spectral indices dCSI and dNDVI provided the next best fits for prediction of stand A_{max} average at 56 days post-fire ($P < 0.001$, AIC: 15.4 and $P < 0.001$, AIC: 15.9, respectively) (Table S10 available as Supplementary data at *Tree Physiology* Online). Spectral index CSI provided the best fit for prediction of stand relative A and F_v/F_m at 56 days post-fire ($P < 0.01$, AIC: 1.7 and $P < 0.05$, AIC: -9.6, respectively) (Figure 5d and f; Tables S4 and S10 available as Supplementary data at *Tree Physiology* Online). Spectral indices NDVI and NBR provided the next best fits for prediction of relative A at 56 days post-fire ($P < 0.001$, AIC: 3.6 and $P < 0.001$, AIC: 4.8, respectively). Spectral indices dNDVI and NDVI provided the next best fits for prediction of F_v/F_m at 56 days post-fire ($P < 0.001$, AIC: -7.5 and $P < 0.001$, AIC: -7.2, respectively) (Table S10, available as Supplementary data at *Tree Physiology* Online).

None of the regression models characterizing the relationship between spectral indices and stand relative A and F_v/F_m was significant at 28 days post-fire (Tables S9 and S10 available as Supplementary data at *Tree Physiology* Online).

Regression relationships between stand mortality and spectral indices that have the lowest AIC values are shown in Figure 6a and b. For *P. monticola*, the regression model with the best fit utilized dNBR for predicting mortality at 28 days post-fire ($P < 0.001$, AIC: 32.8) and RdNBR at 56 days post-fire ($P < 0.001$, AIC: 24.7) (Figure 6a; Tables S3, S4, S9 and S10 available as Supplementary data at *Tree Physiology* Online). Spectral indices RdNBR and SWIR2-SWIR1 band ratio provided the next best fits at 28 days post-fire for prediction of mortality ($P < 0.001$, AIC: 34.3 and $P < 0.001$, AIC: 38.3, respectively), and dNBR and CSI provided the next best fits at 56 days post-fire for prediction of mortality ($P < 0.001$, AIC: 27.6 and $P < 0.001$, AIC: 28.4, respectively) (Tables S9 and S10 available as Supplementary data at *Tree Physiology* Online). For *P. menziesii*, the regression model with the best fit utilized dCSI for prediction of mortality at 28 days post-fire ($P < 0.001$, AIC: 43.4) and at 56 days post-fire ($P < 0.001$, AIC: 46.2) (Figure 6b; Tables S3, S4, S9 and S10 available as Supplementary data at *Tree Physiology* Online). Spectral indices CSI and SWIR2-NIR band ratio provided the next best fits for prediction of mortality at 28 days post-fire ($P < 0.001$, AIC: 45.1 and $P < 0.001$, AIC: 47.2, respectively) and at 56 days post-fire ($P < 0.001$, AIC: 47.9 and $P < 0.001$, AIC: 47.9, respectively) (Tables S9 and S10 available as Supplementary data at *Tree Physiology* Online).

Discussion

This study used a dose–response approach to assess fire intensity impacts on short-term physiological performance in

P. monticola and *P. menziesii* saplings. The hypothesis that increasing fire intensity results in decreased physiological performance and increased mortality was confirmed, although large differences in physiological response were observed between the two species. *Pinus monticola* had lower mortality and less change in physiological performance at lower fire intensities compared with *P. menziesii*, indicating a higher fire resistance of *P. monticola* at this life stage. Likewise, the hypothesis that changes in physiological performance could be detected using spectral indices derived from spectral reflectance at the individual and stand scales was also supported, although relationships were stronger at the individual level than for sapling stands. When considered with prior studies (e.g., Sparks et al. 2016), these findings indicate that spectral reflectance may provide accurate information about physiological performance (Smith et al. 2016, Varner et al. 2021). This is important as it suggests that assessments of fire effects in research and forest management can move beyond current methods that rely on subjective ocular estimates of foliage discoloration and mortality that are difficult to assess at stand and landscape scales (Hood et al. 2018*a*, Varner et al. 2021).

Sapling responses to FRE dose

There were several key differences between the two species in terms of physiological performance response to FRE dose. Generally, *P. monticola* saplings maintained greater physiological performance after higher FRE doses than *P. menziesii* saplings. Some *P. monticola* saplings maintained positive photosynthetic rates 28 days after the highest FRE doses, whereas, *P. menziesii* saplings had near-zero photosynthesis rates at FRE doses above 0.6 MJ m^{-2} (Figures 2a and 3a). Likewise, chlorophyll fluorescence was maintained at higher FRE doses in *P. monticola* saplings at 28 days post-fire versus *P. menziesii* saplings, indicating either there was less damage to the photosynthetic apparatus or that the saplings enacted repairs following the fires (Figures 2d and 3d). This result in *P. monticola* is similar to the results observed for *P. contorta* var. *latifolia* (Smith et al. 2017), where chlorophyll fluorescence in saplings rapidly fell following intense fires (FRE = 1.2 MJ m^{-2}) but then recovered and was maintained for 2 weeks prior to a significant reduction that led to sapling mortality. Together, these results suggest that these two *Pinus* species prioritize resource allocation to repair the photosynthetic apparatus. This is an interesting result given that these two *Pinus* species are not closely related (Gernandt et al. 2005).

Pinus monticola also exhibited larger reductions in A_{max} at lower FRE doses, compared with chlorophyll fluorescence (Figure 2). It is likely that fire-affected saplings closed stomata quickly after the fire treatments to reduce water loss, as evidenced by the decline in g_s in Figure 2c. As photosynthesis relies on the adequate conductance of water and carbon dioxide, stomatal closure would result in the immediate

reduction of photosynthesis. In comparison, the downregulation of photosynthesis, or the breakdown of proteins and pigments in the light harvesting and electron transport that is assessed by chlorophyll fluorescence, is a slower process that may explain why F_v/F_m did not decrease substantially until 56 days post-fire. Prolonged reductions in g_s could result from decreases in water conductivity due to heat-induced embolism in the xylem (Michaletz et al. 2012, West et al. 2016, Bär et al. 2018). However, studies that use actual fires and not fire proxies have not found evidence of reduced hydraulic conductivity in other similarly aged conifer saplings subjected to surface fires of similar intensity (Partelli-Feltrin et al. 2021, 2023). Instead, extensive damage to the phloem was observed and saplings saw reduced nonstructural carbohydrates (sugars and starches) in the stem and roots (Partelli-Feltrin et al. 2023). If the same phloem dysfunction occurred in our study, accumulation of starch in chloroplasts could have also caused downregulation of photosynthesis, through feedback inhibition (Kozlowski and Pallardy 1997, Myers et al. 1999). This could occur with no reduction in water supplied to the foliage, while capacity to conduct photosynthesis assessed by fluorescence would be unaffected. Other potential factors driving reduced photosynthesis include reduced conductance of water, carbon dioxide and other nutrients within and among cells due to heat-induced damage to leaf structure. Internal leaf structure can strongly affect carbon dioxide conductance (Flexas et al. 2012), thus any structural change, such as heat-induced cellular deformation (Michaletz et al. 2012), could potentially reduce photosynthesis.

Differences in physiological performance between species subjected to fires of the same intensity may also be attributed to differences in specific leaf area or the ratio of projected leaf area to leaf mass. Objects with higher surface area to volume ratios have greater heat transfer rates and can heat up more quickly (Finney et al. 2015). Likewise, foliage with a higher specific leaf area may absorb heat such that levels capable of damaging the photosynthetic apparatus are met more quickly than in foliage with lower specific leaf area (Knight and Ackerly 2003). A cross-comparison of FRE–A_{max} dose–response relationships in conifer saplings also provides some evidence for this hypothesis (Figure 7a). Specifically, relationships with steeper declines in photosynthesis at lower FRE doses are apparent in some species with higher specific leaf areas (*P. monticola* and *L. occidentalis*) compared with those with lower specific leaf areas (*P. ponderosa* and *P. contorta*) (Figure 7a).

Foliage structure and arrangement in the crown may also play a role in fire-induced damage and changes in physiological performance. Many *Pinus* species tend to have 'clumps' or 'tufts' of foliage surrounding terminal branch buds (Fournier et al. 1996, Thies et al. 2005, Keeley 2012). In this study, needles in the inner positions of these tufts tended to survive and have higher A_{max} and g_s rates and chlorophyll fluorescence. On the
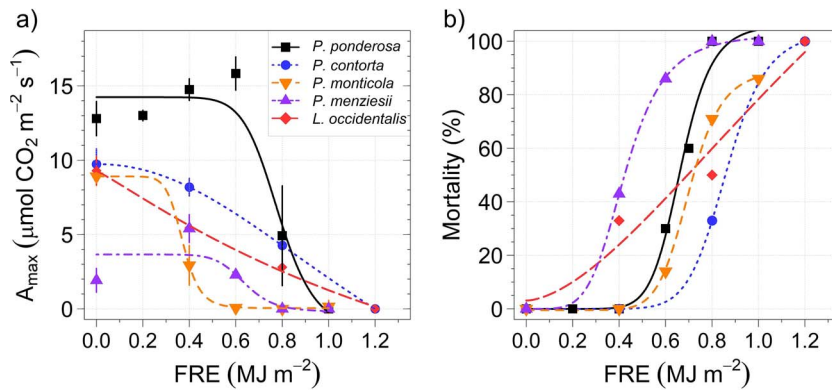
Figure 7. Dose–response relationships between FRE and A_{max} (a) and FRE and mortality (b) at 28 days post-fire for 2- to 3-year-old saplings representing three different *Pinus* species, *Pseudotsuga menziesii* and *Larix occidentalis*. Error bars in (a) represent SE ($n = 5$). *Pinus ponderosa* (Dougl. ex Laws.) data are from Steady et al. (2019) and *Pinus contorta* (Douglas) and *L. occidentalis* (Nutt.) data are from Smith et al. (2017).

contrary, *P. menziesii* needles do not have this tuft structure, and saplings could have sustained more consistent heat-induced damage across the crown, leading to lower photosynthesis rates and chlorophyll fluorescence. Additionally, *P. menziesii* terminal branch buds are much smaller and more exposed than *P. monticola* buds and likely sustained more heat-induced damage during the fire treatments. Similar to foliage, smaller buds can heat up to lethal temperatures more quickly than larger buds (Michaletz and Johnson 2006) and could lead to higher bud necrosis in a tree crown during the sporadic, short-duration heat pulses experienced in fires (Kremens et al. 2010). This is important as partial or complete bud necrosis reduces a tree's ability to produce new foliage and would require adequate nonstructural carbohydrate stores and mobilization for maintenance respiration, as well as osmotic and defense needs (McDowell et al. 2011, Hood et al. 2018a).

The effects observed for these saplings may not apply to older, larger trees. Fire impacts on tree physiology and mortality depend largely on tree size (McDowell et al. 2018), with smaller trees generally being most vulnerable to fire. Fire-resistant traits in older and larger *P. monticola* and *P. menziesii* have had time to mature and include thick bark that insulates the stem from heat, high crowns that reduce flame contact with heat-sensitive foliage and a large non-structural carbohydrate reserve allocated to post-fire recovery and maintenance (Starker 1934, Vanderweide and Hartnett 2011, He et al. 2012, Keeley 2012).

Despite these differences between mature trees and saplings, knowledge of how saplings respond to fire is critically needed. In the western United States, prescribed fires are used for reducing surface fuel load, tree density and crown fire hazard (Battaglia et al. 2009), and greater usage is expected in forest management plans (Kolden 2019, Hiers et al. 2020, Prichard et al. 2021). Dose–response curves like those produced in this study, and other studies (Figure 7), are useful to esti-mate the fire intensity needed to reduce sapling mortality for desired species and/or increase mortality of undesired species

(Smith et al. 2017, Steady et al. 2019). Relations of this form are also widely used within fire-enabled Earth system models, potentially enabling improvements to predicting dynamic vege-tation responses to fire and how they may impact the carbon cycle (Hanan et al. 2022, Shuman et al. 2022).

Physiological performance quantification using spectral indices

The quantification of physiological performance in these two species using common spectral indices is promising and builds off prior research that has shown similar results in different species. In this study, spectral indices based on wavelengths mainly sensitive to foliar pigments (CCI, PRI, NDVI and their differenced formulations) were the best predictors of photo-synthetic performance (Figure 4; Table S1 and S2 available as Supplementary data at *Tree Physiology* Online). Prior studies have found that spectral indices such as CCI and PRI that utilize wavelengths sensitive to carotenoid leaf pigments are more accurate proxies of photosynthesis than are indices such as NDVI which are sensitive to chlorophyll (Gamon et al. 2016, Wong et al. 2019). This difference is largely because carotenoid pigments, given their photoprotective and antioxidant roles, increase in foliage when plants are stressed (Gamon et al. 2016), while chlorophyll levels can remain stable during similar levels of stress (Wong et al. 2019). This means that conifers can have periodic reductions in photosynthetic rate due to changes in environmental conditions (e.g., water stress), while light absorption remains constant (Grace et al. 2007, Peñuelas et al. 2011). However, other studies have found that NDVI can be an accurate proxy for post-fire photosynthetic performance because the NIR wavelengths it uses are sensitive to leaf structural changes that occur with increasing fire intensity (Sparks et al. 2016). Overall, changes in foliar pigment com-position and damage to internal leaf structure after fire remain key knowledge gaps in assessing fire impacts on physiological performance.

The ability to accurately quantify physiological performance using spectral indices is also promising because repeated observations could be used to identify early indicators of tree mortality (Sperry and Love 2015, Hood et al. 2018a). For example, declining trends in spectral indices sensitive to live forest canopy cover have been used to identify and map forest canopy cover loss due to stressors such as drought, insects and disease (Cohen et al. 2016, Huo et al. 2019, Moreno-Fernandez et al. 2021). Metrics derived from time series data, such as the slope, variability and maximum change, could be used to parameterize predictive mortality models (Huo et al. 2019). Individual tree crown mortality classification has been demonstrated using single-date high resolution multispectral imagery acquired via unmanned aerial vehicles (UAVs) (Bergmüller and Vanderwel 2022). Repeated observations using similar platforms (e.g., UAVs, airborne sensors) could provide the necessary time series data for predicting tree death.

In general, individual sapling measurements provided more accurate quantification of physiological performance than sapling stand measurements. At the stand scale, spectral indices utilizing NIR wavelengths (e.g., CSI, NDVI, SWIR2NIR band ratio) typically captured very high physiological performance and very low physiological performance. This could be because live crown area, when viewed at nadir, was reduced to similar proportions across the dose groups, especially in groups exposed to FRE doses higher than 0.4 MJ m^{-2} (Figure 1). Near infrared (NIR) reflectance is highly sensitive to leaf structure (Ollinger 2011), where leaves exposed to lower levels of heat reflect more NIR than leaves exposed to high doses of heat (Sparks et al. 2016), possibly due to intra-leaf cellular deformation (Michaletz et al. 2012) and dehydration (Sinclair et al. 1973). Additionally, background reflectance from sapling branches, soil and char may have obscured any reflectance signal from live foliage, except in cases where live foliage dominated the sensor field-of-view. These results indicate that physiological performance is likely best assessed at the individual tree crown level to minimize confounding influences. However, given the low stand measurement sample size in this study, future work should explore stand-level characterization using a larger sample size. High-resolution imagery (e.g., < 2 m spatial resolution) and multi-spectral LiDAR collected from airplanes and UAVs may provide adequate data for individual tree crown characterization, given prior studies have used such data for foliage chemical content estimation, species identification and crown level mortality (Asner et al. 2015, Budei et al. 2018, Bergmüller and Vanderwel 2022).

The accurate characterization of stand-level mortality using spectral indices indicates that high-to-moderate spatial resolution imagery may provide adequate mortality estimation at stand to landscape scales. The best performing indices incorporated NIR and SWIR wavelengths (e.g., dNBR, RdNBR, CSI, SW2SW1), which has also been observed in studies that quantified post-fire tree mortality using spectral indices derived from Landsat data (Whitman et al. 2018, Harvey et al. 2019, Furniss et al. 2020). Concurrent reductions in NIR reflectance and increases in SWIR reflectance have been observed in tree foliage exposed to higher doses of heat (Sparks et al. 2016), likely resulting from changes in leaf structure and reductions in leaf water content in damaged and dead foliage (Ollinger 2011). The accuracy of indices that use NIR and SWIR wavelengths, along with the sigmoidal form of the relationships between spectral indices and tree mortality, has been observed elsewhere, including in studies that use Landsat-derived spectral indices (Furniss et al. 2020).

Conifer sapling cross-comparison

A cross-comparison of the FRE to A_{max}/mortality dose–response curves in saplings of similar age and size from different studies to date are shown in Figure 7. Saplings are generally considered to represent a worst-case scenario in terms of how much fire intensity dose is needed to cause mortality, as they have not had enough time to develop fire-resistant features such as thick bark and high crowns (Smith et al. 2017, 2018). It is likely that bark thickness for the saplings in Figure 7 was similar, and differences in the dose–response curves are likely owing to differences in crown structure and damage (Engber and Varner 2012). These combined results however raise the question of whether the common 100% survival for *Pinus* species at FRE dosages of 0.4 MJ m^{-2} (Figure 7b) could indicate the presence of a functional trait associated across the *Pinus* genus to fully survive low intensity fires common in *Pinus*-dominated stands (Hudak et al. 2016, Sparks et al. 2017). Above these survival thresholds, each of the studied *Pinus* species exhibits very similar sigmoid responses, with complete mortality generally occurring around 1 MJ m^{-2}. As noted in Steady et al. (2019), the thresholds of survival and mortality will generally shift to the right with increasing age and size of the trees, and Smith et al. (2017) hypothesized that stressors may lead to the thresholds shifting to the left. However, we hypothesize that even if the curves shift, the shape of the curves may remain the same and that size/age-based and stressor correction factors could be created to translate these curves into ecosystem and Earth-system models.

Conclusions

Understanding how fire impacts tree physiology and mortality is important for informing fire effects modeling and natural resource management. However, the majority of fire effects studies do not quantify the heat flux that a tree receives during a fire, limiting their ability to identify mechanisms of tree injury and mortality and/or predict fire effects. This study advances our understanding of how fire affects tree physiology and mortality by utilizing a novel dose–response approach to assess physiological performance in saplings subjected to surface fires

of varying intensity. Our findings demonstrate the higher fire resistance of *P. monticola* compared with *P. menziesii* at this life stage, given the ability of *P. monticola* saplings to maintain higher photosynthesis and chlorophyll fluorescence at higher doses, and lower mortality at lower fire intensity doses. The assessment of physiological performance using remotely sensed spectral reflectance advances the fire effects quantification status quo beyond subjective ocular estimates of dead and dying foliage. Results show that common vegetation indices can accurately characterize physiological performance at the individual crown scale (e.g., PRI, CCI, NDVI), and accurately characterize mortality at the stand scale (e.g., NBR, CSI, RdNBR). These results suggest that current high spatial resolution sensors on airborne and UAV platforms could utilize such spectral indices for tree crown-level assessments. Furthermore, repeated observations may help identify early indicators of tree death, such as decreasing trends or high variability in spectral index values over time.

The conifer sapling cross-comparison showed consistent high survivorship of *Pinus* species at low FRE doses, which is consistent with the close evolutionary relationship between fire and the radiation of the genus (He et al. 2012). However, detailed dose–response experiments have only been conducted on a handful of species. Clearly, prior to a definitive conclusion regarding a potential *Pinus* functional trait, more research is warranted on a larger selection of pines, including species with documented sensitivity to low levels of fire intensity (e.g., *Pinus albicaulis*, *Pinus contorta* var. *murrayana*, *Pinus flexilis*; Cope 1993, Johnson 2001, Fryer 2002). It is unknown how consistent such patterns are across pines or conifers more broadly, let alone how such patterns compare across angiosperm trees. Ultimately, the conifer cross-comparison highlights the utility of using dose–response experiments not only for understanding physiology and mortality responses to fire, but also as a guide for natural resource managers seeking to reduce or increase sapling mortality for desired or undesired species.

Supplementary data

Supplementary data for this article are available at *Tree Physiology* Online.

Conflict of interest

None declared.

Funding

Data availability

All data can by obtained upon request to the authors.

References

Abatzoglou JT, Battisti DS, Williams AP, Hansen WD, Harvey BJ, Kolden CA (2021) Projected increases in western US forest fire despite growing fuel constraints. Comm Earth Environ 2:1–8.

Agee JK (1993) Fire ecology of Pacific Northwest forests. Island Press, Washington, DC.

Akaike H (1974) A new look at the statistical model identification. IEEE Trans Auto Control 19:716–723.

Anderegg WR, Chegwidden OS, Badgley G, Trugman AT, Cullenward D, Abatzoglou JT, Hicke JA, Freeman J, Hamman JJ (2022) Future climate risks from stress, insects and fire across US forests. Ecol Lett 25:1510–1520.

Asner GP, Martin RE, Anderson CB, Knapp DE (2015) Quantifying forest canopy traits: imaging spectroscopy versus field survey. Remote Sens Environ 158:15–27.

Bär A, Nardini A, Mayr S (2018) Post-fire effects in xylem hydraulics of *Picea abies*, *Pinus sylvestris* and *Fagus sylvatica*. New Phytol 217:1484–1493.

Bär A, Michaletz ST, Mayr S (2019) Fire effects on tree physiology. New Phytol 223:1728–1741.

Battaglia M, Smith FW, Shepperd WD (2009) Predicting mortality of ponderosa pine regeneration after prescribed fire in the Black Hills, South Dakota, USA. Int J Wildland Fire 18:176–190.

Battipaglia G, Savi T, Ascoli D, Castagneri D, Esposito A, Mayr S, Nardini A (2016) Effects of prescribed burning on ecophysiological, anatomical and stem hydraulic properties in *Pinus pinea* L. Tree Physiol 36:1019–1031.

Bergmüller KO, Vanderwel MC (2022) Predicting tree mortality using spectral indices derived from multispectral UAV imagery. Remote Sens 14:2195.

Berner LT, Law BE, Meddens AJ, Hicke JA (2017) Tree mortality from fires, bark beetles, and timber harvest during a hot and dry decade in the western United States (2003–2012). Environ Res Lett 12:065005.

Bison NN, Partelli-Feltrin R, Michaletz ST (2022) Trait phenology and fire seasonality co-drive seasonal variation in fire effects on tree crowns. New Phytol 234:1654–1663.

Bonan GB (2008) Forests and climate change: forcings, feedbacks, and the climate benefits of forests. Science 320:1444–1449.

Bornkamp B, Pinheiro J, Bretz F (2022) DoseFinding: planning and analyzing dose finding experiments. R package version 1.0-2. Available online: http://www.cran.r-project.org/web/packages/DoseFinding/ (8 August 2022, date last accessed).

Brodersen CR, Germino MJ, Johnson DM et al. (2019) Seedling survival at timberline is critical to conifer mountain forest elevation and extent. Front For Glob Change 2:9.

Budei BC, St-Onge B, Hopkinson C, Audet FA (2018) Identifying the genus or species of individual trees using a three-wavelength airborne lidar system. Remote Sens Environ 204:632–647.

Burns RM, Honkala BH (1990) Silvics of North America: conifers. Volume 1. US Department of Agriculture, Forest Service, Agriculture Handbook 654, Washington, DC.

Butler BW, Dickinson MB (2010) Tree injury and mortality in fires: developing process-based models. Fire Ecol 6:55–79.

Carter GA (1998) Reflectance wavebands and indices for remote estimation of photosynthesis and stomatal conductance in pine canopies. Remote Sens Environ 63:61–72.

Choudhury BJ (1987) Relationships between vegetation indices, radiation absorption, and net photosynthesis evaluated by a sensitivity analysis. Remote Sens Environ 22:209–233.

Cohen WB, Yang Z, Stehman SV, Schroeder TA, Bell DM, Masek JG, Huang C, Meigs GW (2016) Forest disturbance across the conterminous United States from 1985–2012: the emerging dominance of forest decline. For Ecol Manage 360:242–252.

Cope AB (1993) *Pinus contorta* var. *murrayana*. In: Fire effects information system. US Department of Agriculture, Forest Service, Rocky Mountain Research Station, Fire Sciences Laboratory (Producer) https://www.fs.usda.gov/database/feis/plants/tree/pinconm/all.html.

Davis KM, Clayton BD, Fischer WC (1980) Fire ecology of Lolo National Forest habitat types. In: US Department of Agriculture, Forest Service, Intermountain Forest and Range Experiment Station INT-79, Ogden, UT.

Engber EA, Varner JM (2012) Predicting Douglas-fir sapling mortality following prescribed fire in an encroached grassland. Restor Ecol 20:665–668.

Epting J, Verbyla D, Sorbel B (2005) Evaluation of remotely sensed indices for assessing burn severity in interior Alaska using Landsat TM and ETM+. Remote Sens Environ 96:328–339.

Finney MA, Cohen JD, Forthofer JM et al. (2015) Role of buoyant flame dynamics in wildfire spread. Proc Natl Acad Sci USA 112:9833–9838.

Fischer WC, Bradley AF (1987) Fire ecology of western Montana forest habitat. US Department of Agriculture. General Technical Report INT-223. Intermountain Research Station, Ogden, UT.

Flexas J, Barbour MM, Brendel O et al. (2012) Mesophyll diffusion conductance to CO_2: an unappreciated central player in photosynthesis. Plant Sci 193:70–84.

Fournier RA, Landry R, August NM, Fedosejevs G, Gauthier RP (1996) Modelling light obstruction in three conifer forests using hemispherical photography and fine tree architecture. Agric For Meteorol 82:47–72.

Fryer JL (2002) *Pinus albicaulis*. In: Fire effects information system. U.S. Department of Agriculture, Forest Service, Rocky Mountain Research Station, Fire Sciences Laboratory (Producer). https://www.fs.usda.gov/database/feis/plants/tree/pinalb/all.html.

Furniss TJ, Kane VR, Larson AJ, Lutz JA (2020) Detecting tree mortality with Landsat-derived spectral indices: improving ecological accuracy by examining uncertainty. Remote Sens Environ 237:111497.

Gamon J, Peñuelas J, Field C (1992) A narrow-waveband spectral index that tracks diurnal changes in photosynthetic efficiency. Remote Sens Environ 41:35–44.

Gamon JA, Huemmrich KF, Wong CY, Ensminger I, Garrity S, Hollinger DY, Noormets A, Peñuelas J (2016) A remotely sensed pigment index reveals photosynthetic phenology in evergreen conifers. Proc Natl Acad Sci USA 113:13087–13092.

Genty B, Briantais JM, Baker NR (1989) The relationship between the quantum yield of photosynthetic electron transport and quenching of chlorophyll fluorescence. Biochim Biophys Acta 990:87–92.

Gernandt DS, Lopez GG, Garcia SO, Liston A (2005) Phylogeny and classification of pines. Taxon 54:29–42.

Grace J, Nichol C, Disney M, Lewis P, Quaife T, Bowyer P (2007) Can we measure terrestrial photosynthesis from space directly, using spectral reflectance and fluorescence? Glob Chang Biol 13:1484–1497.

Griffith RS (1992) *Pinus monticola*. In: Fire effects information system. US Department of Agriculture, Forest Service, Rocky Mountain Research Station, Fire Sciences Laboratory. https://www.fs.usda.gov/database/feis/plants/tree/pinmot/all.html.

Hanan EJ, Kennedy MC, Ren J, Johnson MC, Smith AMS (2022) Missing climate feedbacks in fire models: limitations and uncertainties in fuel loadings and the role of decomposition in fine fuel accumulation. J Adv Mod Earth Syst 12:e2021MS002818.

Harvey BJ, Andrus RA, Anderson SC (2019) Incorporating biophysical gradients and uncertainty into burn severity maps in a temperate fire-prone forested region. Ecosphere 10:e02600.

He T, Pausas JG, Belcher CM, Schwilk DW, Lamont BB (2012) Fire-adapted traits of Pinus arose in the fiery cretaceous. New Phytol 194:751–759.

Hiers JK, O'Brien JJ, Varner JM et al. (2020) Prescribed fire science: the case for a refined research agenda. Fire Ecol 16:1–15.

Hood S, Abrahamson I, Cansler CA (2018a) Fire resistance and regeneration characteristics of Northern Rockies tree species. In: Fire effects information system. US Department of Agriculture, Forest Service, Rocky Mountain Research Station, Missoula Fire Sciences Laboratory. https://www.fs.fed.us/database/feis/pdfs/other/FireResistRegen.html.

Hood SM, Varner JM, Van Mantgem P, Cansler CA (2018b) Fire and tree death: understanding and improving modeling of fire-induced tree mortality. Environ Res Lett 13:113004.

Hudak AT, Dickinson MB, Bright BC, Kremens RL, Loudermilk EL, O'Brien JJ, Ottmar HBS (2016) Measurements relating fire radiative energy density and surface fuel consumption–RxCADRE 2011 and 2012. Int J Wildland Fire 25:25–37.

Huo LZ, Boschetti L, Sparks AM (2019) Object-based classification of forest disturbance types in the conterminous United States. Remote Sens 11:477.

Jiménez E, Vega JA, Fernández C (2017) Response of *Pinus pinaster* Ait. trees to controlled localized application of heat to stem and crown. Trees 31:1203–1213.

Johnson KA (2001) *Pinus flexilis*. In: Fire effects information system. US Department of Agriculture, Forest Service, Rocky Mountain Research Station, Fire Sciences Laboratory (Producer). https://www.fs.usda.gov/database/feis/plants/tree/pinfle/all.html.

Jones JL, Webb BW, Butler BW, Dickinson MB, Jimenez D, Reardon J, Bova AS (2006) Prediction and measurement of thermally induced cambial tissue necrosis in tree stems. Int J Wildland Fire 15:3–17.

Jolly WM, Cochrane MA, Freeborn PH, Holden ZA, Brown TJ, Williamson GJ, Bowman DM (2015) Climate-induced variations in global wildfire danger from 1979 to 2013. Nat Commun 6:1–11.

Keeley JE (2009) Fire intensity, fire severity and burn severity: a brief review and suggested usage. Int J Wildland Fire 18:16–126.

Keeley JE (2012) Ecology and evolution of pine life histories. Ann For Sci 69:445–453.

Key CH, Benson NC (2006) Landscape assessment: ground measure of severity, the composite burn index; and remote sensing of severity, the normalized burn ratio. General Technical Report RMRS-GTR-164-CD. USDA Forest Service, Rocky Mountain Research Station, Ogden, UT.

Knight CA, Ackerly DD (2003) Evolution and plasticity of photosynthetic thermal tolerance, specific leaf area and leaf size: congeneric species from desert and coastal environments. New Phytol 160:337–347.

Kolden CA (2019) We're not doing enough prescribed fire in the western United States to mitigate wildfire risk. Fire 2:30.

Kremens RL, Smith AM, Dickinson MB (2010) Fire metrology: current and futuredirections in physics-based measurements. Fire Ecol 6:13–35.

Kozlowski TT, Pallardy SG (1997) Physiology of woody plants. Academic Press, San Diego, CA.

Kushla JD, Ripple WJ (1998) Assessing wildfire effects with Landsat thematic mapper data. Int J Remote Sens 19:2493–2507.

Loehman RA, Clark JA, Keane RE (2011) Modeling effects of climate change and fire management on western white pine (*Pinus monticola*) in the northern Rocky Mountains, USA. Forests 2: 832–860.

McCarley TR, Kolden CA, Vaillant NM, Hudak AT, Smith AMS, Wing BM, Kellogg BS, Kreitler J (2017) Multi-temporal LiDAR and Landsat quantification of fire-induced changes to forest structure. Remote Sens Environ 191:419–432.

McDowell NG, Beerling DJ, Breshears DD, Fisher RA, Raffa KF, Stitt M (2011) The interdependence of mechanisms underlying climate-driven vegetation mortality. Trends Ecol Evol 26:523–532.

McDowell NG, Michaletz ST, Bennett KE, Solander KC, Xu C, Maxwell RM, Middleton RS (2018) Predicting chronic climate-driven disturbances and their mitigation. Trends Ecol Evol 33:15–27.

Michaletz ST, Johnson EA (2006) A heat transfer model of crown scorch in forest fires. Can J For Res 36:2839–2851.

Michaletz ST, Johnson EA (2007) How forest fires kill trees: a review of the fundamental biophysical processes. Scand J Forest Res 22:500–515.

Michaletz ST, Johnson EA, Tyree MT (2012) Moving beyond the cambium necrosis hypothesis of post-fire tree mortality: cavitation and deformation of xylem in forest fires. New Phytol 194: 254–263.

Miller JD, Thode AE (2007) Quantifying burn severity in a heterogeneous landscape with a relative version of the delta normalized burn ratio (dNBR). Remote Sens Environ 109:66–80.

Moreno-Fernandez D, Viana-Soto A, Camarero JJ, Zavala MA, Tijerin J, Garcia M (2021) Using spectral indices as early warning signals of forest dieback: the case of drought-prone *Pinus pinaster* forests. Sci Total Environ 793:148578.

Myers DA, Thomas RB, DeLucia EH (1999) Photosynthetic responses of loblolly pine (*Pinus taeda*) needles to experimental reduction in sink demand. Tree Physiol 19:235–242.

Norum RA (1976) Fire intensity-fuel reduction relationships associated with understory burning in larch/Douglas-fir stands. In: Komarek EV Sr 'Proceedings of Tall Timbers Fire Ecology Conference Number 14 and Intermountain Fire Research Council Fire & Land Management Symposium', 8–10 October 1974, Missoula, MT. Tall Timbers Research Station, Proceedings Number FC14, Tallahassee, FL: Tall Timbers Fire Ecology Conference, pp 359–372.

O'Brien JJ, Hiers JK, Varner JM, Hoffman CM, Dickinson MB, Michaletz ST, Loudermilk EL, Butler BW (2018) Advances in mechanistic approaches to quantifying biophysical fire effects. Curr For Rep 4:161–177.

Ollinger SV (2011) Sources of variability in canopy reflectance and the convergent properties of plants. New Phytol 189:375–394.

Oswalt SN, Smith WB, Miles PD, Pugh SA (2019) Forest resources of the United States, 2017: a technical document supporting the Forest Service 2020 RPA Assessment. Gen. Tech. Rep. WO-97. US Department of Agriculture, Forest Service, Washington Office, Washington, DC.

Partelli-Feltrin R, Johnson DM, Sparks AM, Adams HD, Kolden CA, Nelson AS, Smith AMS (2020) Drought increases vulnerability of *Pinus ponderosa* saplings to fire-induced mortality. Fire 3:56.

Partelli-Feltrin R, Smith AMS, Adams HD, Kolden CA, Johnson DM (2021) Short-and long-term effects of fire on stem hydraulics in *Pinus ponderosa* saplings. Plant Cell Environ 44:696–705.

Partelli-Feltrin R, Smith AMS, Adams HD, Thompson RA, Kolden CA, Yedinak KM, Johnson DM (2023) Death from hunger or thirst? Phloem death, rather than xylem hydraulic failure, as a driver of fire-induced conifer mortality. New Phytol 237:1154–1163.

Peñuelas J, Garbulsky MF, Filella I (2011) Photochemical reflectance index (PRI) and remote sensing of plant CO2 uptake. New Phytol 191:596–599.

Peterson DL, Arbaugh MJ (1986) Post-fire survival in Douglas-fir and lodgepole pine: comparing the effects of crown and bole damage. Can J For Res 16:1175–1179.

Pinheiro J, Bates D (2022) Nlme: linear and nonlinear mixed effects models. R package version. Vol. 3, pp. 1–159. https://CRAN.R-project.org/package=nlme (8 August 2022, date last accessed).

Prichard SJ, Hessburg PF, Hagmann RK et al. (2021) Adapting western North American forests to climate change and wildfires: 10 common questions. Ecol App 31:e02433.

R Core Team (2022) R: A Language and Environment for Statistical Computing. R Foundation for Statistical Computing, Vienna, Austria.

Rouse JW, Haas RH, Schell JA, Deering DW, Harlan JC (1974) Monitoring the vernal advancements and retrogradation of natural vegetation. NASA/GSFC, Final Report: Greenbelt, MD, USA, p 137.

Ryan KC, Peterson DL, Reinhardt ED (1988) Modeling long-term fire-caused mortality of Douglas fir. For Sci 41:190–199.

Sayer MAS, Tyree MC, Kuehler EA, Jackson JK, Dillaway DN (2020) Physiological mechanisms of foliage recovery after spring or fall crown scorch in young longleaf pine (*Pinus palustris* Mill.). Forests 11:208.

Schultz CA, McCaffrey SM, Huber-Stearns HR (2019) Policy barriers and opportunities for prescribed fire application in the western United States. Int J Wildland Fire 28:874–884.

Shuman JK, Balch JK, Barnes RT et al. (2022) Reimagine fire science for the Anthropocene. PNAS Nexus 1:115.

Sinclair TR, Schreiber MM, Hoffer RM (1973) Diffuse reflectance hypothesis for the pathway of solar radiation through leaves 1. Agron J 65:276–283.

Smith AMS, Wooster MJ, Drake NA, Dipotso FM, Falkowski MJ, Hudak AT (2005) Testing the potential of multi-spectral remote sensing for retrospectively estimating fire severity in African Savanna environments. Remote Sens Environ 97:92–115.

Smith AMS, Tinkham WT, Roy DP, Boschetti L, Kremens RL, Kumar SS, Sparks AM, Falkowski MJ (2013) Quantification of fuel moisture effects on biomass consumed derived from fire radiative energy retrievals. Geophys Res Lett 40:6298–6302.

Smith AMS, Kolden CA, Tinkham WT et al. (2014) Remote sensing the vulnerability of vegetation in natural terrestrial ecosystems. Remote Sens Environ 154:322–337.

Smith AMS, Sparks AM, Kolden CA et al. (2016) Towards a new paradigm in fire severity research using dose–response experiments. Int J Wildland Fire 25:158–166.

Smith AMS, Talhelm AF, Johnson DM et al. (2017) Effects of fire radiative energy density dose on *Pinus contorta* and *Larix occidentalis* seedling physiology and mortality. Int J Wildland Fire 26: 82–94.

Smith AMS, Kolden CA, Bowman DMJS (2018) Biomimicry can help humans to sustainably coexist with fire. Nat Ecol Evol 2:1827–1829.

Sparks AM, Kolden CA, Talhelm AF, Smith AMS, Apostol KG, Johnson DM, Boschetti L (2016) Spectral indices accurately quantify changes in seedling physiology following fire: towards mechanistic assessments of post-fire carbon cycling. Remote Sens (Basel) 8: 572.

Sparks AM, Smith AMS, Talhelm AF, Kolden CA, Yedinak KM, Johnson DM (2017) Impacts of fire radiative flux on mature *Pinus ponderosa* growth and vulnerability to secondary mortality agents. Int J Wildland Fire 26:95–106.

Sparks AM, Talhelm AF, Feltrin RP, Smith AMS, Johnson DM, Kolden CA, Boschetti L (2018) An experimental assessment of the impact of drought and fire on western larch injury, mortality and recovery. Int J Wildland Fire 27:490–497.

Sperry JS, Love DM (2015) What plant hydraulics can tell us about responses to climate-change droughts. New Phytol 207: 14–27.

Starker TJ (1934) Fire resistance in the forest. J For 32:462–467.

Steady WD, Partelli Feltrin R, Johnson DM et al. (2019) The survival of *Pinus ponderosa* saplings subjected to increasing levels of fire behavior and impacts on post-fire growth. Fire 2:23.

Steinberg PD (2002) *Pseudotsuga menziesii* var. *glauca*. In: Fire effects information system. US Department of Agriculture, Forest Service, Rocky Mountain Research Station, Fire Sciences Laboratory. https://www.fs.usda.gov/database/feis/plants/tree/psemeng/all.html.

Thies WG, Westlind DJ, Loewen M (2005) Season of prescribed burn in ponderosa pine forests in eastern Oregon: impact on pine mortality. Int J Wildland Fire 14:223–231.

Thomas SC, Winner WE (2002) Photosynthetic differences between saplings and adult trees: an integration of field results by meta-analysis. Tree Physiol 22:117–127.

Trigg S, Flasse S (2000) Characterizing the spectral-temporal response of burned savannah using in situ spectroradiometry and infrared thermometry. Int J Remote Sens 21:3161–3168.

Trigg S, Flasse S (2001) An evaluation of different bi-spectral spaces for discriminating burned shrub-savannah. Int J Remote Sens 22:2641–2647.

Tyukavina A, Potapov P, Hansen MC et al. (2022) Global trends of Forest loss due to fire from 2001 to 2019. Front Remote Sens 3:825190.

VanderWeide BL, Hartnett DC (2011) Fire resistance of tree species explains historical gallery forest community composition. For Ecol Manage 261:1530–1538.

Varner JM, Hood SM, Aubrey DP et al. (2021) Tree crown injury from wildland fires: causes, measurement and ecological and physiological consequences. New Phytol 231:1676–1685.

Wallin KF, Kolb TE, Skov KR, Wagner MR (2003) Effects of crown scorch on ponderosa pine resistance to bark beetles in northern Arizona. Environ Entomol 32:652–661.

West AG, Nel JA, Bond WJ, Midgley JJ (2016) Experimental evidence for heat plume-induced cavitation and xylem deformation as a mechanism of rapid post-fire tree mortality. New Phytol 211:828–838.

Whitman E, Parisien MA, Thompson DK, Hall RJ, Skakun RS, Flannigan MD (2018) Variability and drivers of burn severity in the northwestern Canadian boreal forest. Ecosphere 9:e02128.

Williams DL (1991) A comparison of spectral reflectance properties at the needle, branch, and canopy level for selected conifer species. Remote Sens Environ 35:79–93.

Wong CY, D'Odorico P, Bhathena Y, Arain MA, Ensminger I (2019) Carotenoid based vegetation indices for accurate monitoring of the phenology of photosynthesis at the leaf-scale in deciduous and evergreen trees. Remote Sens Environ 233:111407.

Wooster MJ, Roberts GJ, Giglio L et al. (2021) Satellite remote sensing of active fires: history and current status, applications and future requirements. Remote Sens Environ 267:112694.